Since January 2020 Elsevier has created a COVID-19 resource centre with free information in English and Mandarin on the novel coronavirus COVID-19. The COVID-19 resource centre is hosted on Elsevier Connect, the company's public news and information website.

Antiviral Research 200 (2022) 105278

Contents lists available at ScienceDirect

Antiviral Research

journal homepage: www.elsevier.com/locate/antiviral

Novel antiviral activity of PAD inhibitors against human beta-coronaviruses HCoV-OC43 and SARS-CoV-2

Selina Pasquero [a], Francesca Gugliesi [a], Gloria Griffante [b], Valentina Dell'Oste [a], Matteo Biolatti [a], Camilla Albano [a], Greta Bajetto [a,c], Serena Delbue [d], Lucia Signorini [d], Maria Dolci [d], Santo Landolfo [a], Marco De Andrea [a,c,*]

[a] Department of Public Health and Pediatric Sciences, University of Turin – Medical School, Turin, Italy
[b] Department of Translational Medicine, University of Piemonte Orientale, Novara, Italy
[c] CAAD Center for Translational Research on Autoimmune and Allergic Disease, University of Piemonte Orientale, Novara Medical School, Italy
[d] Department of Biomedical, Surgical and Dental Sciences, University of Milan, Milan, Italy

ARTICLE INFO

Keywords:
SARS-CoV-2
HCoV-OC43
Coronavirus
Citrullination
Peptidyl-arginine deiminases
Host-targeting antivirals

ABSTRACT

The current SARS-CoV-2 pandemic, along with the likelihood that new coronavirus strains will appear in the nearby future, highlights the urgent need to develop new effective antiviral agents. In this scenario, emerging host-targeting antivirals (HTAs), which act on host-cell factors essential for viral replication, are a promising class of antiviral compounds. Here we show that a new class of HTAs targeting peptidylarginine deiminases (PADs), a family of calcium-dependent enzymes catalyzing protein citrullination, is endowed with a potent inhibitory activity against human beta-coronaviruses (HCoVs). Specifically, we show that infection of human fetal lung fibroblasts with HCoV-OC43 leads to enhanced protein citrullination through transcriptional activation of PAD4, and that inhibition of PAD4-mediated citrullination with either of the two pan-PAD inhibitors Cl-A and BB-Cl or the PAD4-specific inhibitor GSK199 curbs HCoV-OC43 replication. Furthermore, we show that either Cl-A or BB-Cl treatment of African green monkey kidney Vero-E6 cells, a widely used cell system to study beta-CoV replication, potently suppresses HCoV-OC43 and SARS-CoV-2 replication. Overall, our results demonstrate the potential efficacy of PAD inhibitors, in suppressing HCoV infection, which may provide the rationale for the repurposing of this class of inhibitors for the treatment of COVID-19 patients.

1. Introduction

In recent years, emerging zoonotic RNA viruses have raised serious public health concerns worldwide. Among them, novel coronaviruses (CoVs) deserve special attention due to their high spillover potential and transmissibility rate, often leading to deadly epidemics across multiple countries, worsened by the lack of effective therapies (Fan et al., 2019).

The *Coronaviridae* family consists of enveloped single-stranded, positive-sense RNA viruses classified into four coronavirus genera: alpha, beta, gamma, and delta. To date, seven human coronaviruses (HCoVs), belonging to the alpha and beta genera, have been identified (Su et al., 2016). HCoV-229E and HCoV-OC43 were first described in 1966 and 1967, respectively, followed by HCoV-NL63 in 2004 and HCoV-HKU1 in 2005. HCoVs generally establish infections in the upper respiratory district—responsible for about 10–30% of common cold cases—, but in vulnerable patients they can also cause bronchiolitis and pneumonia (Leao et al., 2020; Paules et al., 2020).

Even though HCoVs have long been recognized as human pathogens, effective treatments against these viruses have only started to be developed after the severe acute respiratory syndrome CoV (SARS-CoV) outbreak in 2002 (Ksiazek et al., 2003; Weiss and Navas-Martin, 2005). Since then, recurrent spillover events from wildlife have led to the appearance of two other highly pathogenic beta-CoV strains associated with severe respiratory diseases in humans: the Middle East respiratory syndrome coronavirus (MERS-CoV) in 2011, which causes MERS (De Wit et al., 2016; Zaki et al., 2012), and the severe acute respiratory syndrome CoV-2 (SARS-CoV-2) in 2019, the etiological agent of the ongoing pandemic of coronavirus disease 2019 (COVID-19) (Lu et al., 2020; Wu et al., 2020).

In this scenario, the widespread vaccine hesitancy, the growing

* Corresponding author. Department of Public Health and Pediatric Sciences, University of Turin – Medical School, Turin, Italy.
E-mail address: marco.deandrea@unito.it (M. De Andrea).

https://doi.org/10.1016/j.antiviral.2022.105278
Received 7 December 2021; Received in revised form 28 February 2022; Accepted 6 March 2022
Available online 11 March 2022

number of breakthroughs among the vaccinated population, the emergence of increasingly infectious SARS-CoV-2 variants, and the likelihood that new CoV strains will continue to appear in the future have all led to the urgent need to develop new antiviral agents able to tackle ongoing SARS-CoV-2 outbreaks. Consistent with this emergency status, HCoV-OC43 has often been used as a surrogate of—or together with—SARS-CoV-2 to test potential inhibitors of HCoV replication in both cell-based assays and *in silico* analysis (Milani et al., 2021).

Most of the approved antiviral drugs are the so-called direct-acting antiviral agents (DAAs), compounds designed against viral proteins deemed essential for infection. For example, remdesivir, whose efficacy against SARS-CoV-2 is highly controversial (Hsu, 2020), and molnupiravir, a new oral antiviral highly effective in preventing severe disease based on the results of a recent Phase 2a trial (Fischer et al., 2021), are nucleoside analogue prodrugs acting as competitive substrates for virally-encoded RNA-dependent RNA polymerase (RdRp) (Beigel et al., 2020; Warren et al., 2016). Another emerging class of antiviral agents named host-targeting antivirals (HTAs) consists of drugs acting on host-cell factors involved in viral replication. To date, most studies have focused on the analysis of viral proteins and the identification of potential DAAs. However, viruses encode a limited number of proteins, and those suitable as drug targets are only a subset of them. Therefore, targeted disruption of the mechanisms devised by HCoVs to manipulate the host cellular environment during infection, such as those leading to immune evasion and host gene expression alterations (Hartenian et al., 2020), holds great promise for the treatment of COVID-19 patients.

Peptidyl-arginine deiminases (PADs) are a family of calcium-dependent enzymes that catalyze a posttranslational modification (PTM) named citrullination, also known as deimination, a process during which the guanidinium group of a peptidyl-arginine is hydrolyzed to form peptidyl-citrulline, an unnatural amino acid (Mondal and Thompson, 2019; Witalison et al., 2015). Five PAD isozymes (PAD 1-4 and 6) are expressed in humans, with a unique distribution in various tissues (Table 1) (Darrah and Andrade, 2018; György et al., 2006; Kanno et al., 2000; Nachat et al., 2005; Slack et al., 2011; Valesini et al., 2015; Vossenaar et al., 2003; Wang and Wang, 2013; Witalison et al., 2015). PAD dysregulation leads to aberrant citrullination, which is a typical biomarker of various inflammatory conditions, suggesting that it may play a pathogenic role in inflammation-related diseases (Acharya et al., 2012; Knight et al., 2015; Sokolove et al., 2013; van Venrooij et al., 2011; Yang et al., 2016; Yuzhalin, 2019).

Given the involvement of PAD in several pathological settings, a number of PAD inhibitors have been synthesized in recent years. Some of these compounds, such as Cl-amidine (Cl-A) and its derivative BB-Cl-amidine (BB–Cl)—in this latter compound the C-terminus is replaced by a benzimidazole to prevent proteolysis of the C-terminal amide, and the N-terminal benzoyl group is replaced by a biphenyl moiety to enhance cellular uptake (Knight et al., 2015)—, can inhibit the activity of all the different isoforms and, as such, are called pan-PAD inhibitors (Falcão et al., 2019; Knight et al., 2015; Knuckley et al., 2010). Other available inhibitors are highly specific for the different PAD-isozymes, like AFM-30 for PAD2 and GSK199 for PAD4 (Table S1) (Lewis et al., 2015; Muth et al., 2017).

In this scenario, a correlation between PAD dysregulation and viral infections has recently emerged. In particular, the antiviral activity of the LL37 protein appears to be compromised upon human rhinovirus (HRV)-induced citrullination (Casanova et al., 2020), and sera from RA patients can specifically recognize artificially citrullinated Epstein-Barr virus (EBV) proteins (Pratesi et al., 2006, 2011; Trier et al., 2018). Consistently, we have recently shown that human cytomegalovirus (HCMV) induces PAD-mediated citrullination of several cellular proteins endowed of antiviral activity, including the two IFN-stimulated genes (ISGs) IFIT1 and Mx1, and that the inhibition of this process by the PAD inhibitor Cl-A blocks viral replication (Griffante et al., 2021). Finally, another recent study has shown that SARS-CoV-2 infection can modulate PADI gene expression, particularly in lung tissues, leading to the intriguing possibility that PAD enzymes may play a critical role in COVID-19 (Arisan et al., 2020).

Based on this evidence, the aim of this work was to ascertain whether PAD inhibitors might constitute a new class of HTAs against HCoVs. For this purpose, we performed cell based-assays to measure the antiviral activity of the previously mentioned both pan- or specific-PAD inhibitors against two members of the beta-CoV genus: HCoV-OC43, the first one to have been discovered, and SARS-CoV-2, the last one to have emerged so far.

Overall, our results show that both HCoV-OC43 and SARS-CoV-2 infections are significantly associated with PAD-mediated citrullination *in vitro*. Importantly, pharmacological inhibition of PAD enzymes through Cl-A treatment led to ~50% reduction of SARS-CoV-2 NP protein expression and 1 log in SARS-CoV-2 yield, suggesting that PAD inhibitors may be considered for repurposing to treat COVID-19.

2. Materials and methods

2.1. Ethics approval statement

Nasal pharyngeal swabs were collected upon approval of the Local Ethics Committee and signature of the informed consent. The

Table 1
Properties of the different human peptidylarginine deiminases (PADs).

	Tissue distribution	Citrullination substrate	Biological process	Disease associated with aberrant citrullination	Reference
PAD1	All living skin layers, hair follicle, uterus, stomach	Keratin and filaggrin	Cornification of epidermal tissue	Psoriasis	Nachat et al. (2005); Senshu et al. (1999); Ying et al. (2009); Zhang et al. (2016)
PAD2	Skeletal muscle, salivary gland, brain, immune cells, bone marrow, skin, peripheral nerves, uterus, spleen, secretory gland, pancreas, kidney, inner ear.	Actin, vimentin, histone, myelin basic protein	Plasticity of the CNS, transcription, regulation, innate immunity and fertility	Multiple sclerosis, rheumatoid arthritis, Alzheimer disease, prion disease	Falcão et al. (2019); Jang et al. (2008); Musse et al. (2008); Vossenaar et al. (2003)
PAD3	Hair follicle, skin, peripheral nerves, CNS	Vimentin, filaggrin, apoptosis inducing factor	Regulation of epidermal function	Unknown	Kanno et al. (2000); Nachat et al. (2005)
PAD4	Immune cells, brain, uterus, joints, bone marrow	Histones, collagen type I, ING4, p300, p21, lamin C, nucleophosmin	Chromatin decondensation, transcription regulation, tumor formation, innate immune response and NETosis process	Rheumatoid arthritis, multiple sclerosis, and cancers	Acharya et al. (2012); Chang et al. (2009); Willis et al. (2017)
PAD6	Ovary, egg cells, embryo, testicle		Oocyte, sperm chromatin decondensation, female productivity, cytoskeleton formation, early fetal growth, and target for contraceptive drugs	Unknown	Esposito et al. (2007); Kan et al. (2011)

Fondazione Ca' Granda, Ospedale Maggiore, Milano, Italy, approved the protocol No. 456_2020 in May 2020.

2.2. Cell lines and viruses

Human lung fibroblast MRC-5 cells (ATCC® CCL-171) and African green monkey kidney Vero-E6 cells (ATCC®-1586) were propagated in Dulbecco's Modified Eagle Medium (DMEM; Sigma) supplemented with 1% (v/v) penicillin/streptomycin solution (Euroclone) and heat-inactivated 10% (v/v) fetal bovine serum (FBS) (Sigma). The human coronavirus strain OC43 (HCoV-OC43) (ATCC® VR-1558) was kindly provided by David Lembo (Department of Clinical and Biological Sciences, University of Turin, Turin, Italy). HCoV-OC43 was propagated on MRC-5 cells at 33 °C in a humidified 5% CO_2 incubator and titrated by standard plaque method on MRC-5 cells, as described elsewhere (Marcello et al., 2020). SARS-CoV-2 was isolated from a nasal-pharyngeal swab positive for SARS-CoV-2. The isolated SARS-CoV-2 strain belongs to the B.1 lineage, carrying the characteristic spike mutation D614G. The B.1 lineage is the large European lineage, the origin of which roughly corresponds to the Northern Italian outbreak in early 2020. The complete nucleotide sequence has been deposited at GenBank and GISAID (accession Nos. MT748758.1 and EPI_ISL 584051, respectively).

2.3. Reagents and treatments

The PAD inhibitors Cl-A, BB-Cl, GSK199, and AFM30a—also known as CAY10723—were purchased from Cayman Chemical (Ann Arbor). All the compounds were solubilized in DMSO according to the manufacturer's instructions. Immediately before use, the inhibitors were diluted in the culture medium to the desired concentrations (Table S1).

2.4. Cell viability assay

MRC-5 or Vero-E6 cells were seeded at a density of 3×10^4/well in a 96-well plate. After 24 h, cells were treated with different PAD inhibitors at the indicated concentrations or with an equal volume of the vehicle alone (DMSO). After 72 h, cell viability was determined by 3-(4,5-dimethylthiazol-2-yl)-2,5-diphenyltetrazolium bromide assay (MTT, Sigma), as previously described (Griffante et al., 2021).

2.5. In vitro antiviral assay

MRC-5 and Vero-E6 cells were cultured in 24-well plates for 1 day and then, 1 h before infection, pre-treated with PAD inhibitors or vehicle alone at the indicated concentrations. Subsequently, cells were infected with HCoV-OC43 at a multiplicity of infection (MOI) of 0.1 or 1. Following virus adsorption (2 h at 33 °C) and viral inoculum removal, new medium with fresh PAD inhibitors or DMSO alone was added to the plates and kept for further 72 h. The extent of HCoV-OC43 replication in MRC-5 cells was assessed by titrating the infectivity of supernatants using plaque assay and comparative real-time RT-PCR. For Vero-E6 cells, the extent of HCoV-OC43 replication was assessed by titrating the infectivity of supernatants using comparative real-time RT-PCR.

SARS-CoV-2 *in vitro* infection of Vero-E6 cells and the anti-viral inhibition assay were conducted as described previously (Parisi et al., 2021).

2.6. Plaque assay

MRC-5 cells were inoculated with 10-fold serial dilutions of the HCoV-OC43. After 24 h, cells were fixed with cold acetone-methanol (50:50) and subjected to indirect immunostaining with an anti-NP-HCoV-OC43 monoclonal antibody (Millipore MAB9012). To determine the virus titer, the number of immunostained foci was counted on each well using the following formula: virus titer (PFU/ml) = number of plaques * 0.1 ml/dilution fold. SARS-CoV-2 plaque assay were performed on VERO-E6 cells as described previously (Parisi et al., 2021).

2.7. Comparative real-time RT-PCR (viral load)

All molecular analyses were performed according to Milewska et al. (2016). Briefly, viral nucleic acids were isolated from 200 μl of sample using the TRI Reagent solution (Sigma-Aldrich), according to the manufacturer's instructions. Extracted viral RNA (4 μl per sample) was retrotranscribed and amplified in a 20 μl reaction mixture containing Sensi Fast Probe No Rox One step kit (Bioline) using a CFX Touch Real Time PCR Detection System (BioRad). The primers and probe for N gene amplification (Eurofins) are reported below:

HCoV-OC43 Fw: AGCAACCAGGCTGATGTCAATACC;

HCoV-OC43 Rv: AGCAGACCTTCCTGAGCCTTCAAT;

Probe (HCoV-OC43P_rt): TGACATTGTCGATCGGGACCCAAGTA (5′ FAM and 3′TAMRA labeled).

The reaction conditions were as follows: 10 min at 45 °C and 20 min at 95 °C, followed by 40 cycles of 5 s at 95 °C and 1 min at 60 °C.

Quantification of SARS-CoV-2 copy numbers in cell supernatants was evaluated *via* specific real time RT-PCR of the *N1* gene, according to the protocols "Coronavirus disease (COVID-19) technical guidance: Laboratory testing for 2019-nCoV in humans" and "CDC 2019-Novel Coronavirus (2019-nCoV) Real-Time RT-PCR Diagnostic Panel", available at: https://www.who.int/emergencies/diseases/novel-coronavirus-2019/technical-guidance/laboratory-guidance and https://www.fda.gov/media/134922/download [last access 25 October 2021]), respectively.

2.8. Cell-associated RNA isolation and quantitative nucleic acid analysis

Total RNA was extracted using the TRI Reagent solution (Sigma-Aldrich), and 1 μg of it retrotranscribed using the RevertAid H-Minus FirstStrand cDNA Synthesis Kit (Thermo Fisher Scientific) according to the manufacturer's instructions. Comparison of mRNA expression between treated and untreated samples was performed by SYBR green-based real time RT-qPCR by Mx3000P apparatus (Santa Clara), using the primers reported previously. As cellular reference, we amplified the housekeeping gene glyceraldehyde-3-phosphate dehydrogenase (GADPH) with the following primers: GAPDH Fw: AGTGGGTGTCGCTGTTGAAGT; GADPH Rv: AACGTGTCAGTGGTGGACCTG. The reaction conditions were as follows: 2 min at 95 °C, followed by 40 cycles of 5 s at 95 °C and 1 min at 60 °C.

2.9. Western blot analysis

MRC-5 or Vero-E6 cells were treated as described in 2.5 and infected at an MOI of 1. The cells were harvested at 48 and 72 hpi, lysed in RIPA buffer (50 mM Tris-HCl, pH 8.0, 1 mM EDTA, 1% Nonidet P-40, 0.1% sodium deoxycholate, 0.1% SDS, 150 mM NaCl), quantified by the Bradford method, and subjected to Western blot analysis. The primary antibodies were as follows: anti-HCoV-OC43 (Millipore MAB9012); anti-PAD1 (ABCAM ab181791); anti-PAD2 (Cosmo Bio SML-ROI002-EX); anti-PAD3 (ABCAM ab50246); anti-PAD4 (ABCAM ab128086); anti-PAD6 (ABCAM ab16480); anti-actin (Sigma Aldrich A2066), anti-SARS-CoV-2 (GeneTex GTX36802).

2.10. Detection of citrullination with rhodamine-phenylglyoxal (Rh-PG)

Whole-cell protein extracts were prepared as described in 2.9. Protein citrullination detection was performed as described previously (Griffante et al., 2021). Briefly, equal amounts of protein were resuspended with 80% trichloroacetic acid and incubated with a rhodamine phenylglyoxal (Rh-PG, Cayman) probe, at a final concentration 0.1 mM, for 30 min. The reaction was quenched with 100 mM L-citrulline for 30 min at 4 °C and then centrifuged at 21100×*g* for 10 min. The pellet was washed with ice-cold acetone and resuspended in 2 X SDS loading dye

for gel electrophoresis. Upon staining with brilliant blue G-colloidal solution (Sigma-Aldrich), gels were imaged (excitation = 532 nm, emission = 580 nm) using Chemidoc Imaging System (Biorad).

2.11. Statistical analysis

All data were analyzed using GraphPad Prism (GraphPad Software, San Diego, CA). All results are presented as means ± SEM. The half-maximal inhibitory concentrations (IC_{50}) and half-maximal cytotoxic concentration (CC_{50}) values were calculated by Quest Graph™ IC50 Calculator (AAT Bioquest, Inc, https://www.aatbio.com/tools/ic50-calculator). The selectivity index (SI) values were calculated as the ratio of CC_{50} and IC_{50} (SI= CC_{50}/IC_{50}). The *P*-value was calculated by comparing between % inhibition of infected-treated samples and % inhibition of infected-untreated samples. One-tailed Student's t-test was used to compare groups. Differences were considered statistically

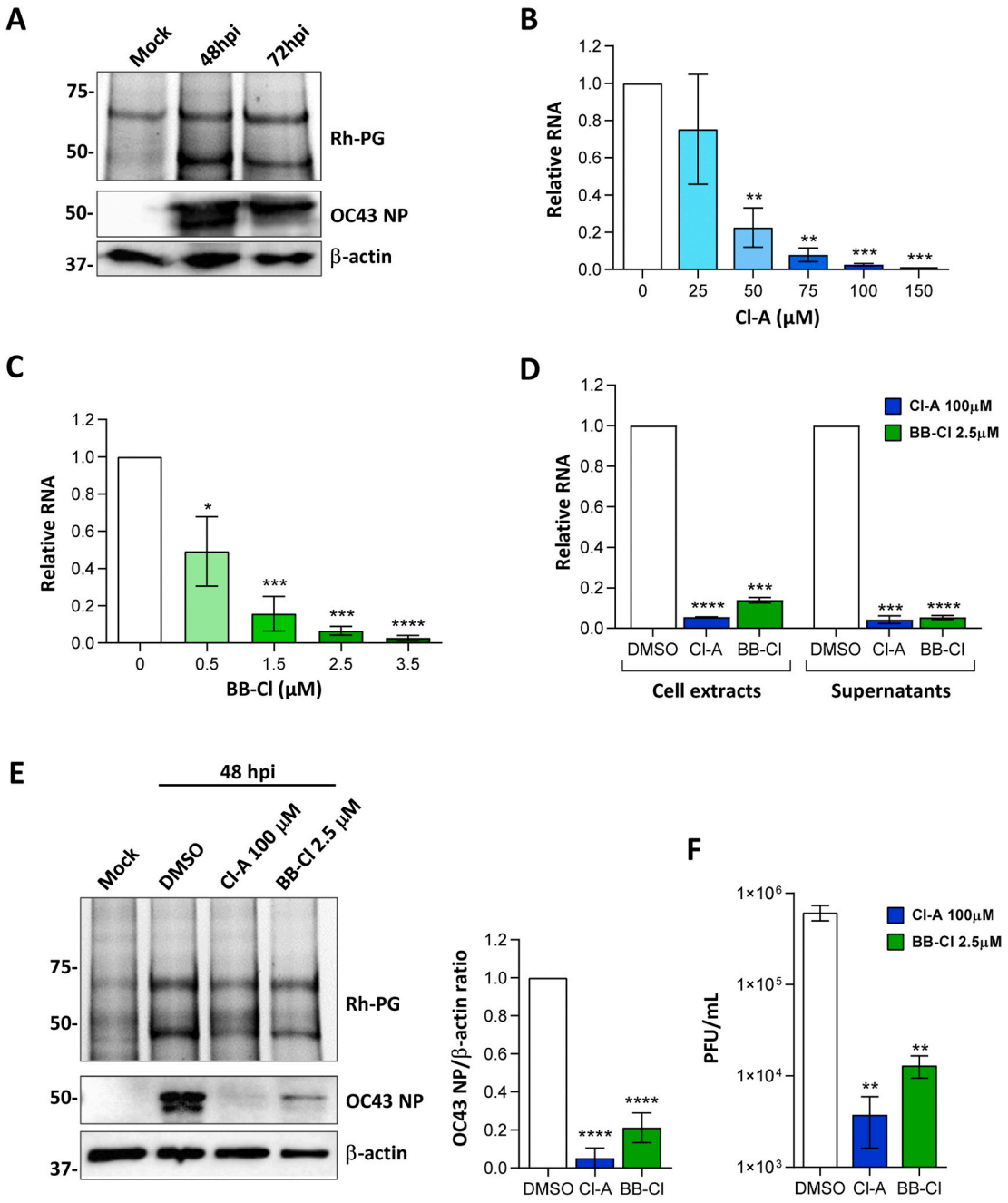

Fig. 1. The pan-PAD inhibitors Cl-A and BB-Cl hamper HCoV-OC43 replication in MRC-5 cells. (A) Rh-PG and Western blot analysis of total protein extract of mock- or HCoV-OC43-infected MRC5 cells (MOI 1). One representative gel of three independent experiments is shown. (B, C) Dose-response curves of the cell-permeable pan-PAD inhibitors Cl-A (B) and BB-Cl (C) in MRC-5 cells infected with HCoV-OC43 (MOI 0.1). After 72 hpi, the viral load was determined by real-time PCR and values were normalized to those for DMSO-treated cells value (0 in the *x* axis) set to 1. Values are expressed as mean ± SEM of three independent experiments. (D) RT-PCR of viral RNA in cell extracts or supernatants from HCoV-OC43-infected MRC5 cells (MOI 0.1) treated with Cl-A (100 μM), BB-Cl (2.5 μM), or DMSO. Values are expressed as mean ± SEM of three independent experiments. (E) Rh-PG and Western blot analysis of protein extract of mock- or HCoV-OC43-infected MRC5 cells (MOI 1) treated with pan-PAD inhibitors as in D. One representative gel of three independent experiments is shown. (F) Viral productions were collected at 72 hpi and analyzed by plaque-forming assay. Values are expressed as mean ± SEM of three independent experiments. $P < 0.05$ (*), <0.01 (**), <0.001 (***) and <0.0001 (****).

significant if $P < 0.05$ (*), $P < 0.01$ (**), $P < 0.001$ (***), and $P < 0.0001$ (****).

3. Results

3.1. Pan-PAD inhibitors block HCoV-OC43 replication in MRC-5 cells

We previously demonstrated that HCMV triggers PAD-mediated citrullination to promote its replication (Griffante et al., 2021). To evaluate whether the protein citrullination profile would also be altered during HCoV infection, we first performed an electrophoresis analysis of protein lysates obtained from MRC-5 lung fibroblasts infected with HCoV-OC43 (MOI 1) incubated with the citrulline-specific probe Rh-PG. At 48 and 72 h post infection (hpi), HCoV-OC43-infected MRC5 cells, but not mock-infected cells, showed a robust increase in total protein citrullination (Fig. 1A). Of note, the expression of the OC43 nucleocapsid protein (OC43 NP) was only detected in HCoV-OC43-infected MRC5 cells, confirming the successful infection of these cells (Fig. 1A).

Next, to test whether PAD enzymatic activity played a functional role in HCoV-OC43 replication, we treated infected cells with the two pan-PAD inhibitors Cl-A and BB-Cl and assessed viral RNA synthesis by real time RT-PCR. Incubation of HCoV-OC43-infected MRC5 cells with increasing amounts of these inhibitors led to a dose-dependent reduction of viral genome copies, a drop that became statistically significant at 50 μM for Cl-A and 0.5 μM for BB-Cl (Fig. 1B and C). The calculated IC_{50}s for Cl-A and BB-Cl were 34.76 μM and 0.54 μM, respectively. To rule out compound cytotoxicity, HCoV-OC43-infected MRC-5 cells were subjected to MTT assay. The results shown in Figs. S1A and B demonstrate that none of the PAD inhibitors significantly reduced cell viability at either IC_{50}. Table 2 shows the CC_{50}s for Cl-A (949.14 μM) and BB-Cl (10.12 μM). Based on the calculated IC_{50} and CC_{50}, the SIs of Cl-A and BB-Cl in HCoV-OC43-infected MRC-5 were quite similar and both greater than 10 (27.3 and 18.6, respectively). Consistent with the results obtained measuring viral RNA, Cl-A and BB-Cl drastically reduced both intra- and extra-cellular viral genome copy numbers (Fig. 1D), confirming the key role of citrullination in HCoV-OC43 replication and viral cycle.

To determine whether PAD inhibition would prevent viral replication and/or production of infectious viral particles, we assessed HCoV-OC43 NP protein expression by Western blotting. We also measured the virus yield by plaque assay using cell extracts and supernatants from HCoV-OC43-infected MRC-5 cells treated with 100 μM Cl-A or 2.5 μM BB-Cl, as previously described. Interestingly, both Cl-A and BB-Cl treatments significantly reduced HCoV-OC43 NP expression in the very same total protein extracts in which a partial suppression of the citrullination profile was also observed by Rh-PG (Fig. 1E). Moreover, consistent with our previous results (Griffante et al., 2021), DMSO treatment alone didn't affect total protein citrullination in uninfected cells nor OC43 N gene expression in infected cells (Figs. S2A and B). Finally, the two drugs significantly reduced PFUs per mL of supernatant by more than 2 and 1 logs, respectively (Fig. 1F).

Table 2
CC50, IC50, and SI of PAD inhibitors against beta-CoVs.

Cell/virus	Compound	IC50[μM]	CC50[μM]	SI
MRC-5/OC43	Cl-amidine	34.80	949.14	27.30
	BB-Cl-amidine	0.53	10.12	18.62
	GSK199	0.60	133.08	224.94
	AFM30a	>20	320.92	>16
Vero-E6/OC43	Cl-amidine	44.15	>1000	>22
	BB-Cl-amidine	10.68	33.06	3.10
Vero-E6/SARS-CoV-2	Cl-amidine	95.17	>1000	>10
	BB-Cl-amidine	17.78	33.06	1.86

3.2. PAD4 plays a central role in HCoV-OC43 replication

To gain more insight into the mechanism of HCoV-OC43-induced cellular citrullination, we asked which of the five known PAD isoforms (PAD1-4 and PAD6) would be preferentially modulated following HCoV-OC43 infection. To answer this question, we performed immunoblot analysis on whole protein lysates obtained from mock and HCoV-OC43-infected MRC5 cells collected at different time points after infection (Fig. 2A). PAD2 and PAD4 were the only two PAD isoforms expressed in these cells, with PAD4 being the only one increased upon infection, as judged by densitometry. By contrast, PAD1, 3, and 6 were neither detectable in mock cells nor did they appear upon infection (Figs. 2A and S5). Given the above results, we next sought to determine whether targeting the enzymatic activity of PAD4 would affect viral replication. To this end, OC43-infected MRC-5 cells were treated with increasing concentrations of the PAD4-specific inhibitor GSK199 or the PAD2-specific inhibitor AFM30a, and assessed for their antiviral activity. Whereas AFM30a treatment only marginally suppressed the HCoV-OC43 replication rate—never exceeding 40% inhibition within the range of concentrations tested (Fig. 2B), exposure of cells to GSK199 robustly inhibited viral genome production in a dose-dependent manner ($IC_{50} = 0.6$ μM), achieving a complete blockade of viral replication at 20 μM (Fig. 2C). Furthermore, MRC-5 cells treated with 20 μM GSK199 were viable, ruling out any unspecific effect due to compound toxicity (Fig. S3). Of note, we could only observe significant cytotoxicity of both compounds at concentrations above 100 μM (Fig. S2). This conferred them an SI > 10, which was particularly robust in the case of GSK199 (224.94) (Table 2).

To confirm these results, we measured the number of viral genome copies in cell lysates and supernatants from MRC-5 cells treated with 20 μM AFM30a or GSK199 and infected with HCoV-OC43. As expected, inhibition of PAD4 by GSK199 drastically reduced the relative viral genome copy number in both compartments compared to vehicle-treated cells, while PAD2 inhibition by AFM30a led to a much less pronounced reduction of viral genome (Fig. 2D). Consistently, immunoblot analysis of total protein extracts from HCoV-OC43-infected MRC-5 cells treated with GSK199 showed a dramatic downregulation of OC43 NP protein expression levels in comparison with vehicle-treated infected cells (Fig. 2E). In contrast, treatment with the PAD2 inhibitor AFM30a only led to a slight decrease in NP protein levels. Fittingly, plaque assay on these cells confirmed a significant reduction of the viral titer in the presence of GSK199 (~2-log reduction), while the inhibitory activity of AFM30a at the same concentration was barely detectable (Fig. 2F).

Taken together, these results suggest that PAD4 plays a major role in HCoV-OC43 replication, and that PAD4 inhibitors are promising anti-HCoV compounds.

3.3. PAD inhibitors affect HCoV-OC43 and SARS-CoV-2 replication in Vero-E6 cells

Since Vero-E6 cells represent a widely used cellular system to study beta-CoV replication in the presence of candidate antiviral compounds, we sought to extend our analysis also to this cell model. Initially, we performed a quantitative analysis of HCoV-OC43 viral RNA production at 72 hpi using different concentrations of Cl-A (50–300 μM) and BB-Cl (5–20 μM). As depicted in Fig. 3, we observed a marked reduction of viral genome replication in Vero-E6 cells treated with either 150–300 μM Cl-A (panel A) or 20 μM BB-Cl (panel B) compared to their vehicle-treated counterparts. These pronounced effects were not a consequence of an intrinsic cytotoxicity of the PAD inhibitors as none of the screened compounds significantly reduced cell viability at the same concentrations as those used in the antiviral assays (Figs. S4A and B and Table 2).

Next, to evaluate whether HCoV-OC43 infection would also trigger protein citrullination in Vero-E6 cells, we performed electrophoresis analysis of protein lysates from HCoV-OC43-infected cells using the Rh-PG probe. As shown in Fig. 3C, cellular protein citrullination in these

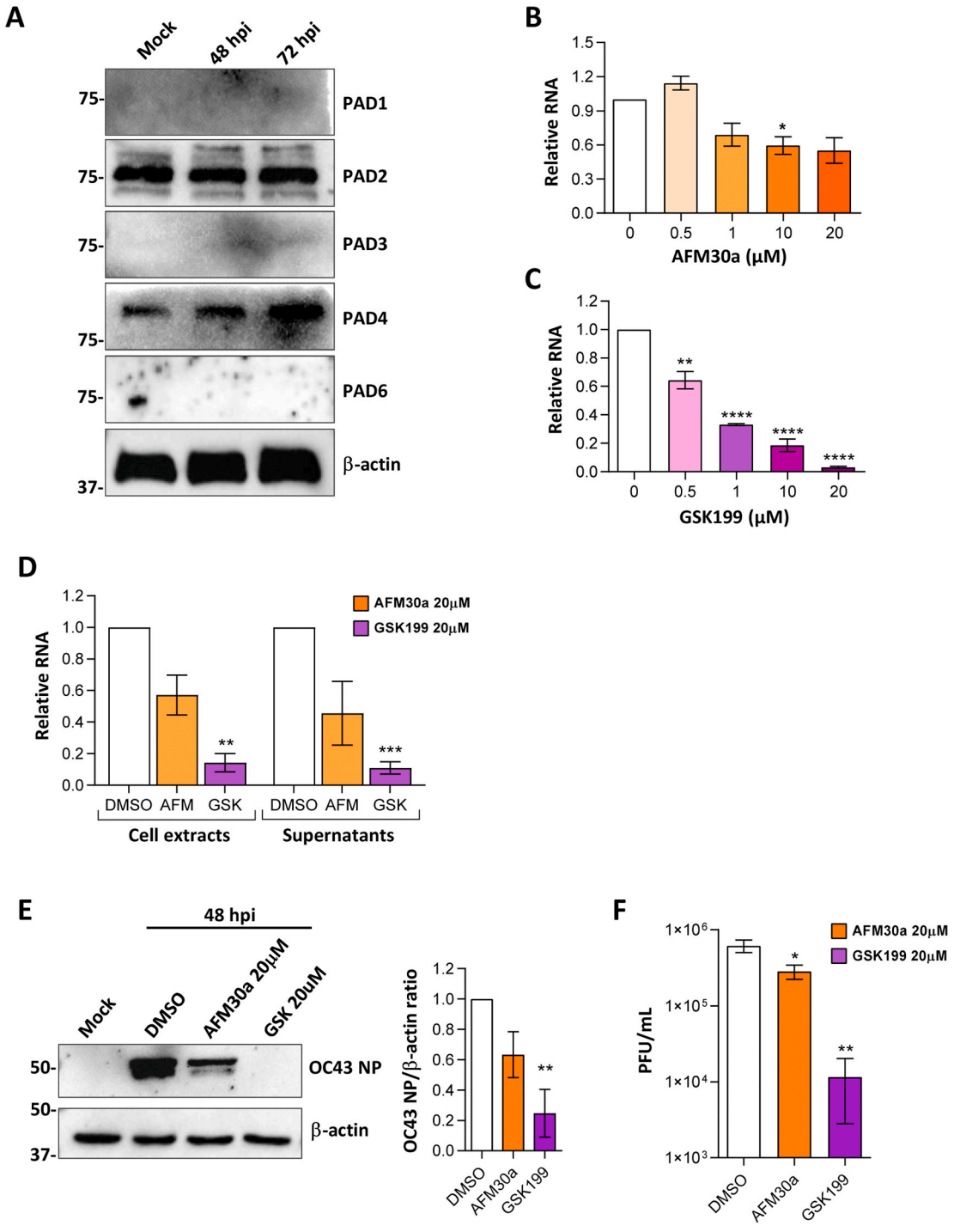

Fig. 2. Effect of PAD2-or PAD4-specific inhibitors on HCoV-OC43 replication in MRC-5 cells. (A) Western blot analysis of protein lysates from mock- or HCoV-OC43-infected MRC5 cells (MOI 1) using antibodies against PAD1, PAD2, PAD3, PAD4, PAD6, or β-actin. The blot shown is representative of three independent experiments. (B–C) Dose-response curves of the cell-permeable pan-PAD inhibitors AFM30a (B) and GSK199 (C) in HCoV-OC43-infected MRC-5 cells (MOI 0.1). After 72 hpi, the viral load was determined by real-time PCR and values were normalized to those for DMSO-treated cells value (0 in the *x* axis) set to 1. Values are represented as mean ± SEM of three independent experiments. (D) Real time RT-PCR on supernatants or cell-associated viral RNA collected from HCoV-OC43-infected MRC5 cells (MOI 0.1) treated with AFM30a (20 μM), GSK199 (20 μM), or DMSO. Values are expressed as mean ± SEM of three independent experiments. (E) Western blot analysis of protein extract of mock- or HCoV-OC43-infected MRC5 cells (MOI 1) treated with AFM30a (20 μM), GSK199 (20 μM), or DMSO. One representative gel of three independent experiments is shown. (F) Viral productions were collected at 72 hpi and analyzed by plaque assay. Values are expressed as mean ± SEM of three independent experiments. $P < 0.05$ (*), <0.01 (**), <0.001 (***) and <0.0001 (****).

infected cells was significantly induced at 48 hpi, whereas it remained almost unchanged in infected cells treated with 300 μM of the Cl-A inhibitor.

To extend our findings to other beta-CoVs, we examined the impact of PAD inhibitors treatment on SARS-CoV-2 viral genome replication. As shown in Fig. 3D and E, both Cl-A and BB-Cl treatments suppressed SARS-CoV-2 viral genome replication in a dose-dependent manner, albeit to a lower extent than that observed for HCoV-OC43.

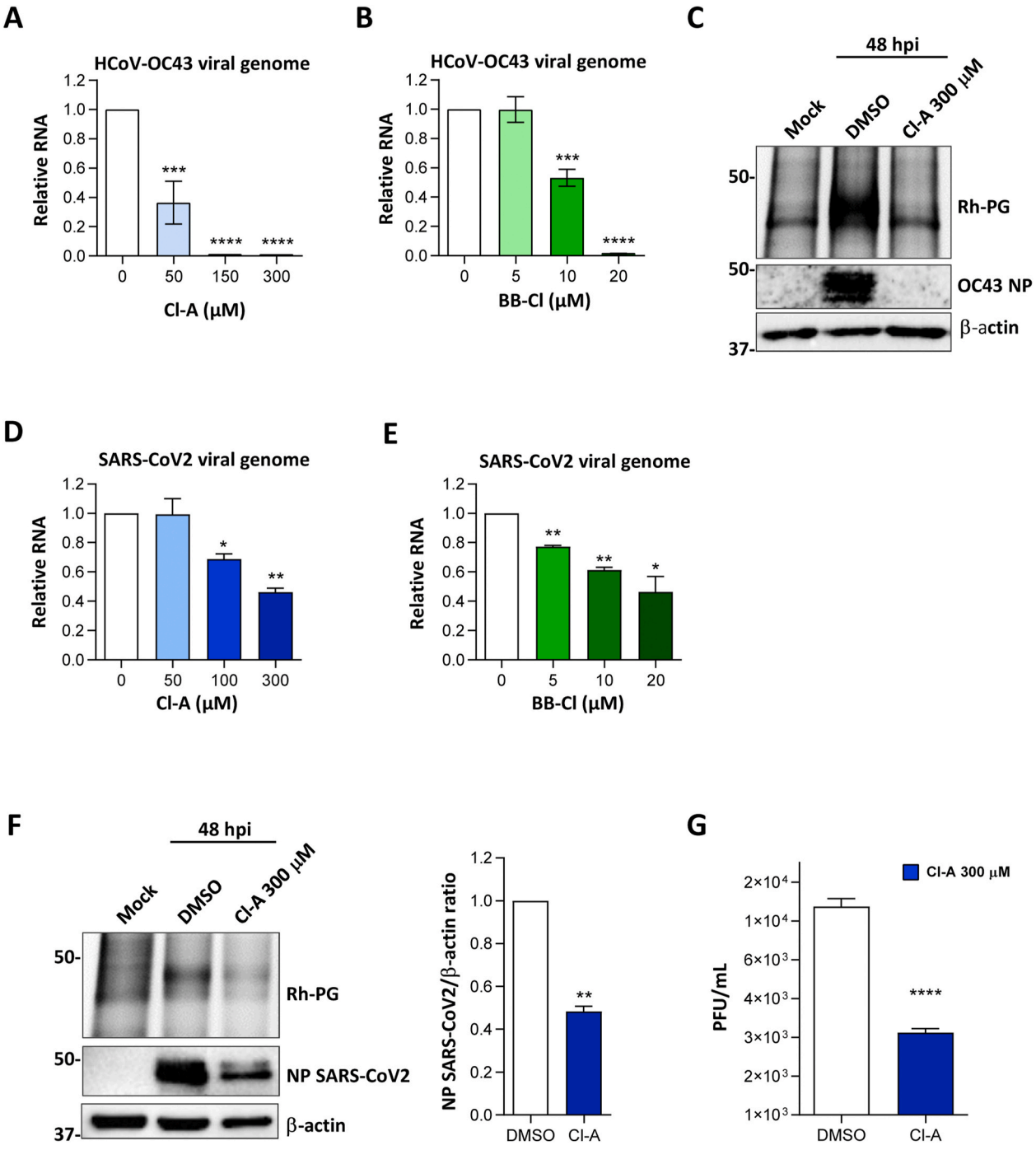

Fig. 3. The pan-PAD inhibitors Cl-A and BB-Cl block β-coronavirus replication in Vero-E6 cells. (A, B) Dose-response curves of the pan-PAD inhibitors Cl-A (A) and BB-Cl (B) in VERO-E6 cells infected with HCoV-OC43 (MOI 0.1). After 72 hpi, the viral load was determined by real-time RT-PCR and values were normalized to those for DMSO-treated cells value (0 in the *x* axis) set to 1. Values represent the mean ± SEM of three independent experiments. (C) Rh-PG and Western blot analysis of total protein extract from mock – or HCoV-OC43-infected VERO-E6 cells (MOI 1) treated with Cl-A (300 μM) or DMSO. One representative gel of three independent experiments is shown. (D, E) Dose-response curves of Cl-A (D) or BB-Cl (E) treatment of SARS-CoV2-infected VERO-E6 cells (MOI 0.1). After 72 hpi, the viral load was determined by real-time RT-PCR and values were normalized to those for DMSO-treated cells value (0 in the *x* axis) set to 1. Values are expressed as mean ± SEM of three independent experiments. (F) Rh-PG and Western blot analysis of total protein extract of mock- or SARS-CoV- infected VERO-E6 cells (MOI 1) and with Cl-A (300 μM) or DMSO. One representative gel of three independent experiments is shown. (G) Viral productions from the same experiment described in F were collected at 72 hpi and analyzed by plaque assay. Values are expressed as mean ± SEM of three independent experiments. $P < 0.05$ (*), <0.01 (**), <0.001 (***) and <0.0001 (****).

To characterize the protein citrullination profile during SARS-CoV-2 infection, protein lysates obtained from Vero-E6 cells infected with SARS-CoV-2, treated with or without Cl-A, were analyzed by Rh-PG (Fig. 3F). The citrullination profile of these SARS-CoV-2-infected cells was consistent with that observed upon HCoV-OC43 infection, both displaying a signal lower than 50 kDa, which specifically appeared after the infection. However, unlike what we observed in HCoV-OC43-infected cells, the citrullination signal, albeit strongly reduced, it never completely disappeared following Cl-A treatment. In line with this observation, Cl-A treatment led to ~50% reduction of SARS-CoV-2 NP

protein expression (Fig. 3F). To corroborate these results, we carried out plaque reduction assays in SARS-CoV-2-infected Vero-E6 cells treated with 300 μM Cl-A as described above. Consistent with our previous results, the inhibition of PAD catalytic activity resulted in a reduction of 1 log in SARS-CoV-2 yield (Fig. 3G).

Altogether, our results demonstrate that beta-CoV infection is associated with protein citrullination. Moreover, treatment of HCoV-OC43 and SARS-CoV-2-infected cells with PAD pan-inhibitors inhibits virus replication restoring the physiological citrullination profile.

4. Discussion

We have recently shown that HCMV infection triggers PAD-mediated citrullination of several host proteins in primary human fibroblasts, and that this activity enhances viral fitness *per se* (Griffante et al., 2021). Here, we extend those findings to two RNA viruses, HCoV-OC43 and SARS-CoV-2, which we demonstrate to be both capable of promoting PAD-mediated citrullination *in vitro*. In particular, we show that HCoV-OC43 infection of MRC-5 lung fibroblasts upregulates total protein citrullination, and that this process is required for optimal viral replication. A similar induction in citrullination levels was also found in CoV-infected Vero-E6 cells, a non-human model system widely used to study HCoVs, especially SARS-CoV-2 (Dittmar et al., 2021; Ghosh et al., 2021; Milani et al., 2021; Wing et al., 2021), suggesting that HCoVs can modulate citrullination across species.

Citrullination is a posttranslational modification mediated by PAD family members, whose distribution and expression patterns are modulated by inflammatory signals in a tissue-specific manner (Table 1) (Acharya et al., 2012; Esposito et al., 2007; Falcão et al., 2019; Kan et al., 2011; Knight et al., 2015; Nachat et al., 2005; Vossenaar et al., 2003; Willis et al., 2011; Yang et al., 2016). Fittingly, we and others have recently reported a positive association between viral infection and PAD-mediated upregulation of citrullination in different cellular models (Arisan et al., 2020; Casanova et al., 2020; Griffante et al., 2021), raising the important question as to whether pharmacological inhibition of PAD activity can be used to reduce viral replication in infected patients. In the present study, we provide additional evidence supporting the use of PAD inhibitors to curb viral growth. Specifically, we show that treatment of HCoV-OC43-infected MRC-5 cells with either of the two pan-PAD inhibitors Cl-A and BB-Cl (Biron et al., 2016; Knight et al., 2015; Ledet et al., 2018; Willis et al., 2011) or the specific PAD4 inhibitor GSK199, but not the PAD2 inhibitor AFM30a, can not only efficiently inhibit viral replication but also reduce the production of infectious particles in the supernatant. This finding is consistent with our observation that MRC-5 cells express basal levels of both PAD2 and PAD4, but only PAD4 is significantly increased upon viral infection. Of note, the considerable reduction in viral replication and titer by the GSK199 compound was achieved at concentrations that do not affect cell viability. Indeed, the high SI of GSK199 (224.94, Table 2) along with its potent antiviral activity makes this PAD4 inhibitor an attractive target for further therapeutic development, a possibility further supported by results showing that targeting PAD4 led to a significant improvement of the clinical and histopathological end-points in a preclinical model of murine arthritis (Willis et al., 2017). This potential therapeutic usefulness would also be supported by a recent study by Arisan and co-workers showing that SARS-CoV-2 infection can modulate PADI gene expression in lung tissues (Arisan et al., 2020). In good agreement, here we show that the inhibitory activity of Cl-A and BB-Cl is not just restricted to HCoV-OC43-infected fibroblasts, but it can also be extended to SARS-CoV-2-infected Vero-E6 cells, highly permissive cells commonly used to propagate and study beta-CoV strains (Ogando et al., 2020). In these cells, both compounds efficiently suppress SARS-CoV-2 genome replication in a dose-dependent manner, albeit at higher concentrations than those used to inhibit HCoV-OC43 replication.

In the past two years, much research has attempted to assess the impact of interferon inducible proteins (ISGs) on SARS-CoV2 infection. In this regard, Banerjee and colleagues have shown that many ISG proteins, including IFIT1 and MX1, are induced during infection, and that their expression reduces virus replication (Banerjee et al., 2021). Interestingly, we have recently shown that the same ISGs are citrullinated by PAD2 and PAD4 during HCMV infection, which hampers their biological activity (Griffante et al., 2021). Therefore, it is possible that PAD inhibitors act by blocking the inactivating citrullination of ISGs by PADs in response to beta-CoV infection, thus restoring the viral restriction activity of ISGs. Nevertheless, it is important to point out that this mechanism would only partially explain the antiviral activity of PAD inhibitors. Indeed, VERO cells have lost the ability to produce IFN due to spontaneous gene deletions (Desmyter et al., 1968, Mosca and Pitha, 1986) and consequently do not express ISG proteins. This loss of IFN responsiveness would however be consistent with the lower efficacy of PAD inhibitors in Vero-E6 *vs.* MRC-5 cells. Experiments are ongoing to test whether this difference is virus- or cell line-dependent.

Another implication of our findings revealing a strong induction of citrullination levels in SARS-CoV-2-infected Vero-E6 cells is that PAD inhibitors may be used to treat COVID-19 patients. It is in fact conceivable to envisage an association between SARS-CoV-2 infection and aberrant citrullination as a way to induce an inflammatory state in different tissues (Delorey et al., 2021).

Another important aspect that supports the repurposing of PAD inhibitors for antiviral therapy is that their efficacy in treating various inflammatory conditions, such as arthritis, colitis, and sepsis, has already been confirmed in preclinical and *in vitro* studies, all showing a good safety profile of such compounds (Chumanevich et al., 2011; Willis et al., 2011; Zhao et al., 2016). Of note, a recent review by Elliot and coworkers explores the possibility that PAD inhibitors, especially PAD4 inhibitors, may be used to resolve SARS-CoV2-induced thrombotic complications (Elliott et al., 2021). Indeed, neutrophil extracellular traps (NETs) and their constituents, including citrullinated histones, display a linear connection with thrombotic manifestations in COVID-19 patients. This intriguing scenario fits quite well with the results presented in the present study since, in a clinical context, the antiviral activity of the PAD inhibitors described here could potentially synergize with their inhibitory effect on immunothrombosis.

In the current pandemic of COVID-19, it is more important than ever that the most promising anti-SARS-CoV-2 drug candidates enter clinical development. Based on some similarities between the clinical outcome observed in autoimmune/autoinflammatory disease and COVID-19, including lung involvement and aberrant cytokine release, pan- and specific-PAD inhibitors—*i.e.*, GSK199—repurposing can be foreseen as a valuable strategy, as it enables to accelerate the use of compounds with already known safety profiles. Moreover, treatments based on molecules with beneficial multi-target activities—a concept known as polypharmacology (Ravikumar and Aittokallio, 2018)—, which may help counteract multiple complications as those observed in COVID-19 patients, may show an increased antiviral spectrum.

In conclusion, our findings unveil an unprecedented role of citrullination in the replication of the two human coronaviruses HCoV-OC43 and SARS-CoV-2 in lung and kidney epithelial cells. We also provide evidence that increased PAD activity is required for β-HCoV replication, highlighting the potential use of PAD inhibitors as novel HTAs against β-HCoV infections. Experiments are ongoing to assess the target citrullinated proteins by proteomics approaches, as well as to test the anti-β-HCoV efficacy and safety of other PAD inhibitors in a wider range of cell lines that can more accurately represent the different tissues where the virus replicates *in vivo*.

Lastly, based on the current availability of different animal models to be exploited for SARS-CoV-2 replication (Lee and Lowen, 2021), including K18-hACE2 transgenic mice challenged with SARS-CoV-2 (Conforti et al., 2021), investigations are being performed to test the feasibility of our drug repurposing strategy *in vivo*.

Declaration of competing interest

The authors declare that they have no known competing financial interests or personal relationships that could have appeared to influence the work reported in this paper.

Acknowledgments

We thank Marcello Arsura for critically reviewing the manuscript. This research was supported by the University of Turin (PoC - TOINPROVE/2020 to M.D.A., RILO2020 and RILO2021 to M.D.A., F.G., V.D.O. and M.B.), by the Ministry of Education, University and Research – MIUR (PRIN Project 2017ALPCM to V.D.O.) and by the AGING Project—Department of Excellence—Department of Translational Medicine, University of Piemonte Orientale (G.G.).

Appendix A. Supplementary data

Supplementary data to this article can be found online at https://doi.org/10.1016/j.antiviral.2022.105278.

References

Acharya, N.K., Nagele, E.P., Han, M., Coretti, N.J., DeMarshall, C., Kosciuk, M.C., Boulos, P.A., Nagele, R.G., 2012. Neuronal PAD4 expression and protein citrullination: possible role in production of autoantibodies associated with neurodegenerative disease. J. Autoimmun. 38, 369–380. https://doi.org/10.1016/j.jaut.2012.03.004.

Arisan, E.D., Uysal-Onganer, P., Lange, S., 2020. Putative roles for peptidylarginine deiminases in COVID-19. Int. J. Mol. Sci. 21, 1–29. https://doi.org/10.3390/ijms21134662.

Banerjee, A., El-Sayes, N., Budylowski, P., Jacob, R.A., Richard, D., Maan, H., Aguiar, J. A., Demian, W.L., Baid, K., D'Agostino, M.R., Ang, J.C., Murdza, T., Tremblay, B.J., Afkhami, S., Karimzadeh, M., Irving, A.T., Yip, L., Ostrowski, M., Hirota, J.A., Kozak, R., Capellini, T.D., Miller, M.S., Wang, B., Mubareka, S., McGeer, A.J., McArthur, A.G., Doxey, A.C., Mossman, K., 2021 May 21. Experimental and natural evidence of SARS-CoV-2-infection-induced activation of type I interferon responses. iScience 24 (5), 102477. https://doi.org/10.1016/j.isci.2021.102477. Epub 2021 Apr 26. PMID: 33937724; PMCID: PMC8074517.

Beigel, J.H., Tomashek, K.M., Dodd, L.E., Mehta, A.K., Zingman, B.S., Kalil, A.C., Hohmann, E., Chu, H.Y., Luetkemeyer, A., Kline, S., Lopez de Castilla, D., Finberg, R. W., Dierberg, K., Tapson, V., Hsieh, L., Patterson, T.F., Paredes, R., Sweeney, D.A., Short, W.R., Touloumi, G., Lye, D.C., Ohmagari, N., Oh, M., Ruiz-Palacios, G.M., Benfield, T., Fätkenheuer, G., Kortepeter, M.G., Atmar, R.L., Creech, C.B., Lundgren, J., Babiker, A.G., Pett, S., Neaton, J.D., Burgess, T.H., Bonnett, T., Green, M., Makowski, M., Osinusi, A., Nayak, S., Lane, H.C., 2020. Remdesivir for the treatment of Covid-19 — final report. N. Engl. J. Med. 383, 1813–1826. https://doi.org/10.1056/nejmoa2007764.

Biron, B.M., Chung, C.-S., O'brien, X.M., Chen, Y., Reichner, J.S., Ayala, A., 2016. In: E-mail Cl-Amidine Prevents Histone 3 Citrullination and Neutrophil Extracellular Trap Formation, and Improves Survival in a Murine Sepsis Model. https://doi.org/10.1159/000448808.

Casanova, V., Sousa, F.H., Shakamuri, P., Svoboda, P., Buch, C., D'Acremont, M., Christophorou, M.A., Pohl, J., Stevens, C., Barlow, P.G., 2020. Citrullination alters the antiviral and immunomodulatory activities of the human cathelicidin LL-37 during rhinovirus infection. Front. Immunol. 11 https://doi.org/10.3389/fimmu.2020.00085.

Chang, X., Han, J., Pang, L., Zhao, Y., Yang, Y., Shen, Z., 2009. Increased PADI4 expression in blood and tissues of patients with malignant tumors. BMC Cancer 9, 40. https://doi: 10.1186/1471-2407-9-40.

Chumanevich, A.A., Causey, C.P., Knuckley, B.A., Jones, J.E., Poudyal, D., Chumanevich, A.P., Davis, T., Matesic, L.E., Thompson, P.R., Hofseth, L.J., 2011. Suppression of colitis in mice by Cl-amidine: a novel peptidylarginine deiminase inhibitor. Am. J. Physiol. Gastrointest. Liver Physiol. 300, G929–G938. https://doi.org/10.1152/ajpgi.00435.2010.

Conforti, A., Marra, E., Palombo, F., Roscilli, G., Ravà, M., Fumagalli, V., Muzi, A., Maffei, M., Luberto, L., Lione, L., Salvatori, E., Compagnone, M., Pinto, E., Pavoni, E., Bucci, F., Vitagliano, G., Stoppoloni, D., Pacello, M.L., Cappelletti, M., Ferrara, F.F., D'Acunto, E., Chiarini, V., Arriga, R., Nyska, A., Di Lucia, P., Marotta, D., Bono, E., Giustini, L., Sala, E., Perucchini, C., Paterson, J., Ryan, K.A., Challis, A.-R., Matusali, G., Colavita, F., Caselli, G., Criscuolo, E., Clementi, N., Mancini, N., Groß, R., Seidel, A., Wettstein, L., Münch, J., Donnici, L., Conti, M., De Francesco, R., Kuka, M., Ciliberto, G., Castilletti, C., Capobianchi, M.R., Ippolito, G., Guidotti, L.G., Rovati, L., Iannacone, M., Aurisicchio, L., 2021. COVID-eVax, an electroporated DNA vaccine candidate encoding the SARS-CoV-2 RBD, elicits protective responses in animal models. Mol. Ther. S1525–0016 (21), 00466 https://doi.org/10.1016/j.ymthe.2021.09.011. –4.

Darrah, E., Andrade, F., 2018. Rheumatoid arthritis and citrullination. Curr. Opin. Rheumatol. 30, 72–78. https://doi.org/10.1097/BOR.0000000000000452.

De Wit, E., Van Doremalen, N., Falzarano, D., Munster, V.J., 2016. SARS and MERS: recent insights into emerging coronaviruses. Nat. Rev. Microbiol. 14, 523–534. https://doi.org/10.1038/nrmicro.2016.81.

Delorey, T.M., Ziegler, C.G.K., Heimberg, G., Normand, R., Yang, Y., Segerstolpe, A., Abbondanza, D., Fleming, S.J., Subramanian, A., Montoro, D.T., Jagadeesh, K.A., Dey, K.K., Sen, P., Slyper, M., Pita-Juárez, Y.H., Phillips, D., Biermann, J., Bloom-Ackermann, Z., Barkas, N., Ganna, A., Gomez, J., Melms, J.C., Katsyv, I., Normandin, E., Naderi, P., Popov, Y.V., Raju, S.S., Niezen, S., Tsai, L.T.-Y., Siddle, K. J., Sud, M., Tran, V.M., Vellarikkal, S.K., Wang, Y., Amir-Zilberstein, L., Atri, D.S., Beechem, J., Brook, O.R., Chen, J., Divakar, P., Dorceus, P., Engreitz, J.M., Essene, A., Fitzgerald, D.M., Fropf, R., Gazal, S., Gould, J., Grzyb, J., Harvey, T., Hecht, J., Hether, T., Jané-Valbuena, J., Leney-Greene, M., Ma, H., McCabe, C., McLoughlin, D.E., Miller, E.M., Muus, C., Niemi, M., Padera, R., Pan, L., Pant, D., Pe'er, C., Pfiffner-Borges, J., Pinto, C.J., Plaisted, J., Reeves, J., Ross, M., Rudy, M., Rueckert, E.H., Siciliano, M., Sturm, A., Todres, E., Waghray, A., Warren, S., Zhang, S., Zollinger, D.R., Cosimi, L., Gupta, R.M., Hacohen, N., Hibshoosh, H., Hide, W., Price, A.L., Rajagopal, J., Tata, P.R., Riedel, S., Szabo, G., Tickle, T.L., Ellinor, P.T., Hung, D., Sabeti, P.C., Novak, R., Rogers, R., Ingber, D.E., Jiang, Z.G., Juric, D., Babadi, M., Farhi, S.L., Izar, B., Stone, J.R., Vlachos, I.S., Solomon, I.H., Ashenberg, O., Porter, C.B.M., Li, B., Shalek, A.K., Villani, A.-C., Rozenblatt-Rosen, O., Regev, A., 2021. COVID-19 tissue atlases reveal SARS-CoV-2 pathology and cellular targets. Nature 595, 107–113. https://doi.org/10.1038/s41586-021-03570-8.

Desmyter, J., Melnick, J.L., Rawls, W.E., 1968. Defectiveness of interferon production and of rubella virus interference in a line of African green monkey kidney cells (Vero). J. Virol. 2 (10), 955–961. https://doi.org/10.1128/JVI.2.10.955-961.1968.

Dittmar, M., Lee, J.S., Whig, K., Segrist, E., Li, M., Kamalia, B., Castellana, L., Ayyanathan, K., Cardenas-Diaz, F.L., Morrisey, E.E., Truitt, R., Yang, W., Jurado, K., Samby, K., Ramage, H., Schultz, D.C., Cherry, S., 2021. Drug repurposing screens reveal cell-type-specific entry pathways and FDA-approved drugs active against SARS-Cov-2. Cell Rep. 35, 108959. https://doi.org/10.1016/j.celrep.2021.108959.

Elliott Jr., W., Guda, M.R., Asuthkar, S., Teluguakula, N., Prasad, D.V.R., Tsung, A.J., Velpula, K.K., 2021. PAD inhibitors as a potential treatment for SARS-CoV-2 immunothrombosis. Biomedicines 9 (12), 1867. https://doi.org/10.3390/biomedicines9121867.

Esposito, G., Vitale, A.M., Leijten, F.P., Strik, A.M., Koonen-Reemst, A.M., Yurttas, P., Robben, T.J., Coonrod, S., Gossen, J.A., 2007. Peptidylarginine deiminase (PAD) 6 is essential for oocyte cytoskeletal sheet formation and female fertility. Mol. Cell. Endocrinol. 273 (1–2), 25–31. https://doi: 10.1016/j.mce.2007.05.005.

Falcão, A.M., Meijer, M., Scaglione, A., Rinwa, P., Agirre, E., Liang, J., Larsen, S.C., Heskol, A., Frawley, R., Klingener, M., Varas-Godoy, M., Raposo, A.A.S.F., Ernfors, P., Castro, D.S., Nielsen, M.L., Casaccia, P., Castelo-Branco, G., 2019. PAD2-Mediated citrullination contributes to efficient oligodendrocyte differentiation and myelination. Cell Rep. 27 (4), 1090–1102 e10. https://doi: 10.1016/j.celrep.2019.03.108.

Fan, Y., Zhao, K., Shi, Z.L., Zhou, P., 2019. Bat coronaviruses in China. Viruses. https://doi.org/10.3390/v11030210.

Fischer, W., Eron, J.J., Holman, W., Cohen, M.S., Fang, L., Szewczyk, L.J., Sheahan, T.P., Baric, R., Mollan, K.R., Wolfe, C.R., Duke, E.R., Azizad, M.M., Borroto-Esoda, K., Wohl, D.A., Loftis, A.J., Alabanza, P., Lipansky, F., Painter, W.P., 2021. Molnupiravir, an Oral Antiviral Treatment for COVID-19. https://doi.org/10.1101/2021.06.17.21258639.

Ghosh, A.K., Miller, H., Knox, K., Kundu, M., Henrickson, K.J., Arav-Boger, R., 2021. Inhibition of human coronaviruses by antimalarial peroxides. ACS Infect. Dis. 7, 1985–1995. https://doi.org/10.1021/acsinfecdis.1c00053.

Griffante, G., Gugliesi, F., Pasquero, S., Dell'Oste, V., Biolatti, M., Salinger, A.J., Mondal, S., Thompson, P.R., Weerapana, E., Lebbink, R.J., Soppe, J.A., Stamminger, T., Girault, V., Pichlmair, A., Oroszlán, G., Coen, D.M., De Andrea, M., Landolfo, S., 2021. Human cytomegalovirus-induced host protein citrullination is crucial for viral replication. Nat. Commun. 12, 1–14. https://doi.org/10.1038/s41467-021-24178-6.

György, B., Tóth, E., Tarcsa, E., Falus, A., Buzás, E.I., 2006. Citrullination: a posttranslational modification in health and disease. Int. J. Biochem. Cell Biol. 38, 1662–1677. https://doi.org/10.1016/j.biocel.2006.03.008.

Hartenian, E., Nandakumar, D., Lari, A., Ly, M., Tucker, J.M., Glaunsinger, B.A., 2020. The molecular virology of coronaviruses. J. Biol. Chem. 295, 12910–12934. https://doi.org/10.1074/jbc.REV120.013930.

Hsu, J., 2020. Covid-19: what now for remdesivir? BMJ 371, m4457. https://doi.org/10.1136/bmj.m4457.

Jang, B., Kim, E., Choi, J.K., Jin, J.K., Kim, J.I., Ishigami, A., Maruyama, N., Carp, R.I., Kim, Y.S., Choi, E.K., 2008. Accumulation of citrullinated proteins by up-regulated peptidylarginine deiminase 2 in brains of scrapie-infected mice: a possible role in pathogenesis. Am. J. Pathol. 173 (4), 1129–1142. https://doi: 10.2353/ajpath.2008.080388.

Kan, R., Yurttas, P., Kim, B., Jin, M., Wo, L., Lee, B., Gosden, R., Coonrod, S.A., 2011. Regulation of mouse oocyte microtubule and organelle dynamics by PADI6 and the cytoplasmic lattices. Dev. Biol. 350 (2), 311–322. https://doi: 10.1016/j.ydbio.2010.11.033.

Kanno, T., Kawada, A., Yamanouchi, J., Yosida-Noro, C., Yoshiki, A., Shiraiwa, M., Kusakabe, M., Manabe, M., Tezuka, T., Takahara, H., 2000. Human peptidylarginine deiminase type III: molecular cloning and nucleotide sequence of the cDNA, properties of the recombinant enzyme, and immunohistochemical localization in human skin. J. Invest. Dermatol. 115 (5), 813–823. https://doi: 10.1046/j.1523-1747.2000.00131.x.

Knight, J.S., Subramanian, V., O'Dell, A.A., Yalavarthi, S., Zhao, W., Smith, C.K., Hodgin, J.B., Thompson, P.R., Kaplan, M.J., 2015. Peptidylarginine deiminase

inhibition disrupts NET formation and protects against kidney, skin and vascular disease in lupus-prone MRL/*lpr* mice. Ann. Rheum. Dis. 74, 2199–2206. https://doi.org/10.1136/annrheumdis-2014-205365.

Knuckley, B., Causey, C.P., Jones, J.E., Bhatia, M., Dreyton, C.J., Osborne, T.C., Takahara, H., Thompson, P.R., 2010. Substrate specificity and kinetic studies of PADs 1, 3, and 4 identify potent and selective inhibitors of protein arginine deiminase 3. Biochemistry 49 (23), 4852–4863. https://doi.org/10.1021/bi100363t.

Ksiazek, T.G., Erdman, D., Goldsmith, C.S., Zaki, S.R., Peret, T., Emery, S., Tong, S., Urbani, C., Comer, J.A., Lim, W., Rollin, P.E., Dowell, S.F., Ling, A.-E., Humphrey, C. D., Shieh, W.-J., Guarner, J., Paddock, C.D., Rota, P., Fields, B., DeRisi, J., Yang, J.-Y., Cox, N., Hughes, J.M., LeDuc, J.W., Bellini, W.J., Anderson, L.J., 2003. A novel coronavirus associated with severe acute respiratory syndrome. N. Engl. J. Med. 348, 1953–1966. https://doi.org/10.1056/nejmoa030781.

Leao, J.C., Gusmao, T.P. de L., Zarzar, A.M., Leao Filho, J.C., Barkokebas Santos de Faria, A., Morais Silva, I.H., Gueiros, L.A.M., Robinson, N.A., Porter, S., Carvalho, A. de A.T., 2020. Coronaviridae—Old Friends, New Enemy! Oral Diseases 0–3. https://doi.org/10.1111/odi.13447.

Ledet, M.M., Anderson, R., Harman, R., Muth, A., Thompson, P.R., Coonrod, S.A., Van de Walle, G.R., 2018. BB-Cl-Amidine as a novel therapeutic for canine and feline mammary cancer via activation of the endoplasmic reticulum stress pathway. BMC Cancer 18, 1–13. https://doi.org/10.1186/s12885-018-4323-8.

Lee, C.-Y., Lowen, A.C., 2021. Animal models for SARS-CoV-2. Curr. Opin. Virol. 48, 73–81. https://doi.org/10.1016/j.coviro.2021.03.009.

Lu, R., Zhao, X., Li, J., Niu, P., Yang, B., Wu, H., Wang, W., Song, H., Huang, B., Zhu, N., Bi, Y., Ma, X., Zhan, F., Wang, L., Hu, T., Zhou, H., Hu, Z., Zhou, W., Zhao, L., Chen, J., Meng, Y., Wang, J., Lin, Y., Yuan, J., Xie, Z., Ma, J., Liu, W.J., Wang, D., Xu, W., Holmes, E.C., Gao, G.F., Wu, G., Chen, W., Shi, W., Tan, W., 2020. Genomic characterisation and epidemiology of 2019 novel coronavirus: implications for virus origins and receptor binding. Lancet 395, 565–574. https://doi.org/10.1016/S0140-6736(20)30251-8.

Lewis, H.D., Liddle, J., Coote, J.E., Atkinson, S.J., Barker, M.D., Bax, B.D., Bicker, K.L., Bingham, R.P., Campbell, M., Chen, Y.H., Chung, C.W., Craggs, P.D., Davis, R.P., Eberhard, D., Joberty, G., Lind, K.E., Locke, K., Maller, C., Martinod, K., Patten, C., Polyakova, O., Rise, C.E., Rüdiger, M., Sheppard, R.J., Slade, D.J., Thomas, P., Thorpe, J., Yao, G., Drewes, G., Wagner, D.D., Thompson, P.R., Prinjha, R.K., Wilson, D.M., 2015. Inhibition of PAD4 activity is sufficient to disrupt mouse and human NET formation. Nat. Chem. Biol. 11 (3), 189–191. https://doi.org/10.1038/nchembio.1735.

Marcello, A., Civra, A., Milan Bonotto, R., Nascimento Alves, L., Rajasekharan, S., Giacobone, C., Caccia, C., Cavalli, R., Adami, M., Brambilla, P., Lembo, D., Poli, G., Leoni, V., 2020. The cholesterol metabolite 27-hydroxycholesterol inhibits SARS-CoV-2 and is markedly decreased in COVID-19 patients. Redox Biol. 36, 101682. https://doi.org/10.1016/j.redox.2020.101682.

Milani, M., Donalisio, M., Bonotto, R.M., Schneider, E., Arduino, I., Boni, F., Lembo, D., Marcello, A., Mastrangelo, E., 2021. Combined in silico and in vitro approaches identified the antipsychotic drug lurasidone and the antiviral drug elbasvir as SARS-CoV2 and HCoV-OC43 inhibitors. Antivir. Res. 189, 105055. https://doi.org/10.1016/j.antiviral.2021.105055.

Milewska, A., Kaminski, K., Ciejka, J., Kosowicz, K., Zeglen, S., Wojarski, J., Nowakowska, M., Szczubiałka, K., Pyrc, K., 2016. HTCC: broad range inhibitor of coronavirus entry. PLoS One 11, 1–17. https://doi.org/10.1371/journal.pone.0156552.

Mondal, S., Thompson, P.R., 2019. Protein arginine deiminases (PADs): biochemistry and chemical biology of protein citrullination. Acc. Chem. Res. 52, 818–832. https://doi.org/10.1021/acs.accounts.9b00024.

Mosca, J.D., Pitha, P.M., 1986. Transcriptional and posttranscriptional regulation of exogenous human beta interferon gene in simian cells defective in interferon synthesis. Mol. Cell Biol. 6 (6), 2279–2283. https://doi.org/10.1128/mcb.6.6.2279-2283.1986.

Musse, A.A., Li, Z., Ackerley, C.A., Bienzle, D., Lei, H., Poma, R., Harauz, G., Moscarello, M.A., Mastronardi, F.G., 2008. Peptidylarginine deiminase 2 (PAD2) overexpression in transgenic mice leads to myelin loss in the central nervous system. Dis. Model. Mech. (4–5), 229–240. https://doi: 10.1242/dmm.000729.

Muth, A., Subramanian, V., Beaumont, E., Nagar, M., Kerry, P., McEwan, P., Srinath, H., Clancy, K., Parelkar, S., Thompson, P.R., 2017. Development of a selective inhibitor of protein arginine deiminase 2. J. Med. Chem. 60 (7), 3198–3211. https://doi.org/10.1021/acs.jmedchem.7b00274.

Nachat, R., Méchin, M.C., Charveron, M., Serre, G., Constans, J., Simon, M., 2005. Peptidylarginine deiminase isoforms are differentially expressed in the anagen hair follicles and other human skin appendages. J. Invest. Dermatol. 125 (1), 34–41. https://doi.org/10.1111/j.0022-202X.2005.23763.x.

Ogando, N.S., Dalebout, T.J., Zevenhoven-Dobbe, J.C., Limpens, R.W.A.L., van der Meer, Y., Caly, L., Druce, J., de Vries, J.J.C., Kikkert, M., Bárcena, M., Sidorov, I., Snijder, E.J., 2020. SARS-coronavirus-2 replication in Vero E6 cells: replication kinetics, rapid adaptation and cytopathology. J. Gen. Virol. 101, 925–940. https://doi.org/10.1099/jgv.0.001453.

Parisi, O.I., Dattilo, M., Patitucci, F., Malivindi, R., Delbue, S., Ferrante, P., Parapini, S., Galeazzi, R., Cavarelli, M., Cilurzo, F., Franzè, S., Perrotta, I., Pezzi, V., Selmin, F., Ruffo, M., Puoci, F., 2021. Design and development of plastic antibodies against SARS-CoV-2 RBD based on molecularly imprinted polymers that inhibit *in vitro* virus infection. Nanoscale 13 (40), 16885–16899. https://doi.org/10.1039/d1nr03727g.

Paules, C.I., Marston, H.D., Fauci, A.S., 2020. Coronavirus infections-more than just the common cold. J. Am. Med. Assoc. https://doi.org/10.1001/jama.2020.0757.

Pratesi, F., Tommasi, C., Anzilotti, C., Chimenti, D., Migliorini, P., 2006. Deiminated Epstein-Barr virus nuclear antigen 1 is a target of anti-citrullinated protein antibodies in rheumatoid arthritis. Arthritis Rheum. 54, 733–741. https://doi.org/10.1002/art.21629.

Pratesi, F., Tommasi, C., Anzilotti, C., Puxeddu, I., Sardano, E., Di Colo, G., Migliorini, P., 2011. Antibodies to a new viral citrullinated peptide, VCP2: fine specificity and correlation with anti-cyclic citrullinated peptide (CCP) and anti-VCP1 antibodies. Clin. Exp. Immunol. 164, 337–345. https://doi.org/10.1111/j.1365-2249.2011.04378.x.

Ravikumar, B., Aittokallio, T., 2018. Improving the efficacy-safety balance of polypharmacology in multi-target drug discovery. Expet Opin. Drug Discov. 13, 179–192. https://doi.org/10.1080/17460441.2018.1413089.

Senshu, T., Akiyama, K., Ishigami, A., Nomura, K., 1999. Studies on specificity of peptidylarginine deiminase reactions using an immunochemical probe that recognizes an enzymatically deiminated partial sequence of mouse keratin K1. J. Dermatol. Sci. 21, 113–126. https://doi: 10.1016/s0923-1811(99)00026-2.

Slack, J.L., Causey, C.P., Thompson, P.R., 2011. Protein arginine deiminase 4: a target for an epigenetic cancer therapy. Cell. Mol. Life Sci. 68, 709–720. https://doi.org/10.1007/s00018-010-0480-x.

Sokolove, J., Brennan, M.J., Sharpe, O., Lahey, L.J., Kao, A.H., Krishnan, E., Edmundowicz, D., Lepus, C.M., Wasko, M.C., Robinson, W.H., 2013. Brief report: citrullination within the atherosclerotic plaque: a potential target for the anti-citrullinated protein antibody response in rheumatoid arthritis. Arthritis Rheum. 65, 1719–1724. https://doi.org/10.1002/art.37961.

Su, S., Wong, G., Shi, W., Liu, J., Lai, A.C.K., Zhou, J., Liu, W., Bi, Y., Gao, G.F., 2016. Epidemiology, Genetic Recombination, and Pathogenesis of Coronaviruses. https://doi.org/10.1016/j.tim.2016.03.003.

Trier, N.H., Holm, B.E., Heiden, J., Slot, O., Locht, H., Lindegaard, H., Svendsen, A., Nielsen, C.T., Jacobsen, S., Theander, E., Houen, G., 2018. Antibodies to a strain-specific citrullinated Epstein-Barr virus peptide diagnoses rheumatoid arthritis. Sci. Rep. 8, 3684. https://doi.org/10.1038/s41598-018-22058-6.

van Venrooij, W.J., van Beers, J.J.B.C., Pruijn, G.J.M., 2011. Anti-CCP antibodies: the past, the present and the future. Nat. Rev. Rheumatol. 7, 391–398. https://doi.org/10.1038/nrrheum.2011.76.

Valesini, G., Gerardi, M.C., Iannuccelli, C., Pacucci, V.A., Pendolino, M., Shoenfeld, Y., 2015. Citrullination and autoimmunity. Autoimmun. Rev. 14, 490–497. https://doi.org/10.1016/j.autrev.2015.01.013.

Vossenaar, E.R., Zendman, A.J.W., Van Venrooij, W.J., Pruijn, G.J.M., 2003. PAD, a growing family of citrullinating enzymes: genes, features and involvement in disease. Bioessays 25, 1106–1118. https://doi.org/10.1002/bies.10357.

Wang, S., Wang, Y., 2013. Peptidylarginine deiminases in citrullination, gene regulation, health and pathogenesis. Biochim. Biophys. Acta 1126–1135. https://doi.org/10.1016/j.bbagrm.2013.07.003, 1829.

Warren, T.K., Jordan, R., Lo, M.K., Ray, A.S., Mackman, R.L., Soloveva, V., Siegel, D., Perron, M., Bannister, R., Hui, H.C., Larson, N., Strickley, R., Wells, J., Stuthman, K. S., Van Tongeren, S.A., Garza, N.L., Donnelly, G., Shurtleff, A.C., Retterer, C.J., Gharaibeh, D., Zamani, R., Kenny, T., Eaton, B.P., Grimes, E., Welch, L.S., Gomba, L., Wilhelmsen, C.L., Nichols, D.K., Nuss, J.E., Nagle, E.R., Kugelman, J.R., Palacios, G., Doerffler, E., Neville, S., Carra, E., Clarke, M.O., Zhang, L., Lew, W., Ross, B., Wang, Q., Chun, K., Wolfe, L., Babusis, D., Park, Y., Stray, K.M., Trancheva, I., Feng, J.Y., Barauskas, O., Xu, Y., Wong, P., Braun, M.R., Flint, M., McMullan, L.K., Chen, S.S., Fearns, R., Swaminathan, S., Mayers, D.L., Spiropoulou, C.F., Lee, W.A., Nichol, S.T., Cihlar, T., Bavari, S., 2016. Therapeutic efficacy of the small molecule GS-5734 against Ebola virus in rhesus monkeys. Nature 531, 381–385. https://doi.org/10.1038/nature17180.

Weiss, S.R., Navas-Martin, S., 2005. Coronavirus pathogenesis and the emerging pathogen severe acute respiratory syndrome coronavirus. Microbiol. Mol. Biol. Rev. 69, 635–664. https://doi.org/10.1128/MMBR.69.4.635-664.2005.

Willis, V.C., Banda, N.K., Cordova, K.N., Chandra, P.E., Robinson, W.H., Cooper, D.C., Lugo, D., Mehta, G., Taylor, S., Tak, P.P., Prinjha, R.K., Lewis, H.D., Holers, V.M., 2017. Protein arginine deiminase 4 inhibition is sufficient for the amelioration of collagen-induced arthritis. Clin. Exp. Immunol. 188, 263–274. https://doi.org/10.1111/cei.12932.

Willis, V.C., Gizinski, A.M., Banda, N.K., Causey, C.P., Knuckley, B., Cordova, K.N., Luo, Y., Levitt, B., Glogowska, M., Chandra, P., Kulik, L., Robinson, W.H., Arend, W. P., Thompson, P.R., Holers, V.M., 2011. N-α-Benzoyl-N5-(2-Chloro-1-Iminoethyl)-l-Ornithine amide, a protein arginine deiminase inhibitor, reduces the severity of murine collagen-induced arthritis. J. Immunol. 186, 4396–4404. https://doi.org/10.4049/jimmunol.1001620.

Wing, P.A.C., Keeley, T.P., Zhuang, X., Lee, J.Y., Prange-Barczynska, M., Tsukuda, S., Morgan, S.B., Harding, A.C., Argles, I.L.A., Kurlekar, S., Noerenberg, M., Thompson, C.P., Huang, K.Y.A., Balfe, P., Watashi, K., Castello, A., Hinks, T.S.C., James, W., Ratcliffe, P.J., Davis, I., Hodson, E.J., Bishop, T., McKeating, J.A., 2021. Hypoxic and pharmacological activation of HIF inhibits SARS-CoV-2 infection of lung epithelial cells. Cell Rep. 35, 109020. https://doi.org/10.1016/j.celrep.2021.109020.

Witalison, E.E., Thompson, P.R., Hofseth, L.J., 2015. Protein arginine deiminases and associated citrullination: physiological functions and diseases associated with dysregulation. Curr. Drug Targets 16, 700–710. https://doi.org/10.2174/1389450116666150202160954.

Wu, F., Zhao, S., Yu, B., Chen, Y.M., Wang, W., Song, Z.G., Hu, Y., Tao, Z.W., Tian, J.H., Pei, Y.Y., Yuan, M.L., Zhang, Y.L., Dai, F.H., Liu, Y., Wang, Q.M., Zheng, J.J., Xu, L., Holmes, E.C., Zhang, Y.Z., 2020. A new coronavirus associated with human respiratory disease in China. Nature 579, 265–269. https://doi.org/10.1038/s41586-020-2008-3.

Yang, L., Tan, D., Piao, H., 2016. Myelin basic protein citrullination in multiple sclerosis: a potential therapeutic target for the pathology. Neurochem. Res. 41, 1845–1856. https://doi.org/10.1007/s11064-016-1920-2.

Ying, S., Dong, S., Kawada, A., Kojima, T., Chavanas, S., Méchin, M.C., Adoue, V., Serre, G., Simon, M., Takahara, H., 2009. Transcriptional regulation of peptidylarginine deiminase expression in human keratinocytes. J. Dermatol. Sci. 53 (1), 2–9. https://doi: 10.1016/j.jdermsci.2008.09.009.

Yuzhalin, A.E., 2019. Citrullination in cancer. Cancer Res. 79, 1274–1284. https://doi.org/10.1158/0008-5472.CAN-18-2797.

Zaki, A.M., van Boheemen, S., Bestebroer, T.M., Osterhaus, A.D.M.E., Fouchier, R.A.M., 2012. Isolation of a novel coronavirus from a man with pneumonia in Saudi Arabia. N. Engl. J. Med. 367, 1814–1820. https://doi.org/10.1056/nejmoa1211721.

Zhang, X., Liu, X., Zhang, M., Li, T., Muth, A., Thompson, P.R., Coonrod, S.A., Zhang, X., 2016. Peptidylarginine deiminase 1-catalyzed histone citrullination is essential for early embryo development. Sci. Rep. 6, 38727. http://doi: 10.1038/srep38727.

Zhao, T., Pan, B., Alam, H.B., Liu, B., Bronson, R.T., Deng, Q., Wu, E., Li, Y., 2016. Protective effect of Cl-amidine against CLP-induced lethal septic shock in mice. Sci. Rep. 6, 36696. https://doi.org/10.1038/srep36696.